Optics and Lasers in Engineering 58 (2014) 48–53

Contents lists available at ScienceDirect

Optics and Lasers in Engineering

journal homepage: www.elsevier.com/locate/optlaseng

Sensor for headspace pressure and H_2O concentration measurements in closed vials by tunable diode laser absorption spectroscopy

Tingdong Cai [a,b], Guishi Wang [a], Zhensong Cao [a], Weijun Zhang [a,*], Xiaoming Gao [a,*]

[a] Key Laboratory of Atmospheric Composition and Optical Radiation, Anhui Institute of Optics and Fine Mechanics, Chinese Academy of Sciences, Hefei 230031, PR China

[b] College of Physics and Electronic Engineering, Jiangsu Normal University, Xuzhou 221116, PR China

ARTICLE INFO

Article history:
Received 20 April 2013
Received in revised form
29 November 2013
Accepted 8 December 2013
Available online 18 February 2014

Keywords:
Tunable diode laser absorption spectroscopy (TDLAS)
Sensor
Headspace analysis
Pressure and H_2O concentration

ABSTRACT

The concentration of H_2O and the pressure in the headspace of vials are simultaneously measured by a tunable diode laser sensor based on absorption spectroscopy techniques. The 7168.437 cm^{-1} spectral line of H_2O is chosen as the sensing transition for its strong absorption strength and being reasonably far away from its neighboring molecular transitions. In order to prevent interference absorption by ambient water vapor in the room air, a difference between the measured signal and the referenced signal is used to calculate the pressure and H_2O concentration in the headspace of vials, eliminating the need for inert gas purges and calibration with known gas. The validation of the sensor is conducted in a static vial, yielding an accuracy of 1.23% for pressure and 3.81% for H_2O concentration. The sensitivity of the sensor is estimated to be about 2.5 Torr for pressure and 400 ppm for H_2O concentration over a 3 cm absorption path length respectively. Accurate measurements for commercial freeze-dried products demonstrate the in-line applications of the sensor for the pharmaceutical industry.

1. Introduction

In today's aseptic manufacturing processes, automated leak detection and container closure integrity testing play an important role in protecting primary containers of finished product against microbial contamination [1,2]. The current growth in sterile biopharmaceutical products brings challenges as well as opportunities to the industry in terms of developing in-process monitoring and control strategies that keep processes in a state of control and minimize the risk of product defects [3]. For many finished sterile products, the most important destabilizing factor is the final residual moisture level in the vials of drugs [4,5]. There exist many traditional techniques and instruments for monitoring the moisture content in the vials, such as the residual gas analysis [6], the electronic hygrometer [7,8], the comparative pressure measurement [9], and the pressure rise measurement [10]. These techniques cannot give direct quantitative insight into the process. Instead, one has to establish the relationship between measurement and actual moisture content of the material *ex-situ* for different material and apparatus. Modern techniques such as the low temperature infrared spectroscopy [11], the visual microscopic observation [12], the low-resolution pulse nuclear magnetic resonance [13], and the X-ray powder diffractometry can give *in-situ* and non-destructive insight [14]. However, they are costly to maintain and difficult to validate.

Tunable diode laser absorption spectroscopy (TDLAS) is a rapid and non-destructive analytical method suitable for *in-situ* measurements of multiple parameters such as the concentration, pressure, temperature, and velocity in various environments [15–18]. The diode laser usually covers parts of the ro-vibrational bands of the relevant molecular species in the near-infrared or mid-infrared spectral regions. Semiconductor diode lasers are attractive sources for practical applications owing to their compactness, availability, robustness, compatibility with an optical fiber technology, and relatively ease of use. TDLAS have also been used to monitor gas parameters and vacuum levels in the headspace of sterile product containers in recent years. For example, For example, TDLAS has been demonstrated for the non-invasive determinations of the water pressure [19], the water vapor mass flow rate [20], the sublimation rate [21], the heat transfer parameters [22], and the oxygen concentration [23]. In order to reduce the influence of ambient gases, most of those systems need inert gas purges or sealed under vacuum. Additionally, reference vials with known concentration and pressure used for system calibration are also needed. All these additional features make system requirements more complicated and expensive. Headspace analyses are also performed based on TDLAS employing frequency modulation spectroscopy (FMS) [24–28]. The FMS scheme can yield a higher sensitivity, but disadvantages with regard to cost

* Corresponding authors. Fax: +86 551 5591560.
E-mail addresses: wjzhang@aiofm.ac.cn (W. Zhang), xmgao@aiofm.ac.cn (X. Gao).

0143-8166/$ - see front matter © 2014 Published by Elsevier Ltd.
http://dx.doi.org/10.1016/j.optlaseng.2013.12.005

and system complexity must be considered. In addition, calibration with known gas is also needed for the FMS scheme. There are only very few sensors for headspace analyses are developed without purge system and calibration. For example, Jenkins et al. developed a diode laser absorption sensor for detecting oxygen concentration in headspace of vials employing a 760 nm Vertical Cavity Surface Emitting Laser and a balanced detection circuit. They performed an experiment to demonstrate the accuracy of the sensor using a cylindrical glass test tube to simulate a vial for pharmaceutical inspection applications, but did not confirm the ability of the sensor for commercial freeze-dried products and in-line applications of the sensor for the pharmaceutical industry [29]. To our knowledge, there has been no sensor capable of simultaneous measurement of headspace pressure and H_2O concentration in closed vial employing direct absorption spectroscopy without inert gas purge system and calibration with known gas.

In the present paper, a sensor for simultaneous measurements of pressure and H_2O vapor concentration in the headspace of vials using TDLAS with a distributed feedback (DFB) diode laser near 1.396 μm is developed. A H_2O transition located near 7168.437 cm^{-1} is selected for the sensor because of its strong absorption strength and isolation from interference of neighboring transitions. Due to the strong absorption of the H_2O transition, the direct absorption scheme is employed for the sensor. This scheme is convenient for operation and good for the simplification of the system. Wavelength scans of the laser produced H_2O direct absorption lineshapes for measurement path and reference path. The pressure and H_2O vapor concentration in the headspace of vials are inferred from the difference between the measured signal and the referenced signal. In this way, the sensor does not need inert gas purges and calibration with known gas. Measurements are first validated in a static vial containing H_2O-Air mixtures over the expected pressure range of 0.01 to 1 atm. The sensitivity of the sensor is estimated through 20 successive pressure and concentration measurements recorded during a 20 min experiment time. In order to illustrate the potential of the sensor for in-line applications, measurements are performed on vials which are placed on a rotary stage to simulate the process of an assembly line. An experiment of headspace analysis for commercial freeze-dried products confirms the sensor's accuracy and potential utility for pharmaceutical industry.

2. Theory

The basic equation of absorption spectroscopy is the Beer–Lambert law [30]. This equation relates the transmitted intensity I_t through a uniform gas medium of length L [cm] to the incident intensity I_0 as

$$\left(\frac{I_t}{I_0}\right)_\nu = \exp[-k_\nu L] \tag{1}$$

where k_ν [cm^{-1}] is the spectral absorption coefficient. For an isolated transition i,

$$k_\nu = P x_{abs} S_i(T) \varphi_\nu \tag{2}$$

where P [atm] is the total pressure, x_{abs} is the mole fraction of the absorbing species, S_i [cm^{-2} atm^{-1}] is the line strength at temperature T [K] of the transition, and φ_ν [cm] is the line-shape function which is normalized such that $\int \varphi_\nu d\nu \equiv 1$. The product $k_\nu L$ is known as the spectral absorbance α_ν:

$$\alpha_\nu = -\ln\left(\frac{I_t}{I_0}\right) = k_\nu L = P x_{abs} S_i(T) \varphi_\nu L. \tag{3}$$

The measured absorbance from the target absorption transition is fitted with the appropriate line shape profile for the environmental conditions and the integrated absorbance is calculated from the fit. The integrated absorbance A_i [cm^{-1}] could be expressed as

$$A_i = \int_{-\infty}^{+\infty} \alpha_\nu d\nu = P x_{abs} S_i(T) L = P_{abs} S_i(T) L \tag{4}$$

The integrated absorbance is directly proportional to species partial pressure P_{abs} (and therefore concentration) at a fixed temperature.

The line-shape function φ_ν is usually approximated using a Voigt profile [31] characterized by the collision-broadened full-width at half maximum (FWHM), $\Delta\nu_C$ [cm^{-1}], and the Doppler FWHM, $\Delta\nu_D$ [cm^{-1}]. The collisional width $\Delta\nu_C$ is proportional to the system pressure in the following way:

$$\Delta\nu_C = P \sum_j x_j 2\gamma_{j-abs} \tag{5}$$

here, γ_{j-abs} is the broadening coefficient due to collisions between perturbing species j and the absorbing species.

In our case, the collisional FWHM from the Voigt profile can be written as

$$\Delta\nu_C = P_{air} 2\gamma_{air} + P_{H_2O} 2\gamma_{H_2O} \tag{6}$$

where γ_{air} is the air-broadening coefficient of the transition and γ_{H_2O} is the self-broadening coefficient of the sample. P_{air} is the partial pressure of the perturber component (here laboratory air) and P_{H_2O} is the partial pressure of water vapor.

P_{air} and P_{H_2O} can be obtained from Eqs. (4) and (6) if the temperature, line strength, and path length are known. Then we can obtain the mole fraction of water vapor, x, since

$$x_{H_2O} = P_{H_2O}/P = P_{H_2O}/(P_{air} + P_{H_2O}) \tag{7}$$

3. Experimental procedure

The experimental setup is shown in Fig. 1. The light source used is a single-mode InGaAsP DFB diode laser (NTT Electronics Corporation) operating in the near-infrared near 1.396 μm. The laser power is ~10 mW, and the typical linewidth is ~2 MHz. Frequency tuning of the diode laser could be controlled by scanning either the temperature (~0.43 cm^{-1}/°C) or the current (~0.02 cm^{-1}/mA). The temperature and current are controlled by ILX Lightwave LDX-3724B laser diode controller, with short-term (1 h) temperature stability <0.004 °C and long-term (24 h) temperature stability <0.01 °C. The calibration of the laser wavelength is made by a wavemeter (EXFO Burleigh Products Group, WA-1500-NIR) with an accuracy of about ± 0.001 cm^{-1}. The laser wavelength is driven by a triangle ramp from a function generator (ShengPu, F-20). The optimum scanning frequency is limited by the re-triggering time of the DAQ hardware and is set as 333 Hz in the experiment.

The emitted radiation is collimated by a lens and divided in two beams by a 1×2 fiber splitter after passing through an optical isolator (Koncent, KISO-S-A-1550, −35 dB): as shown in Fig. 1, the first beam (~70% of the power) goes through the headspace of vial along its radial direction, while the second one (~30% of the power) passes through an open path in the ambient air. Both beams are then collected by two homemade InGaAs-PIN photodiodes. In order to minimize the difference between two detectors, the gain of the detectors were adjusted to yield almost the same voltages from the same light before experiment. In the experiment, the two signals are named as measured signal (from the first beam) and referenced signal (from the second beam) respectively. The detector used to acquire the referenced signal is fixed on a sliding guide and the length of the open path in the ambient air

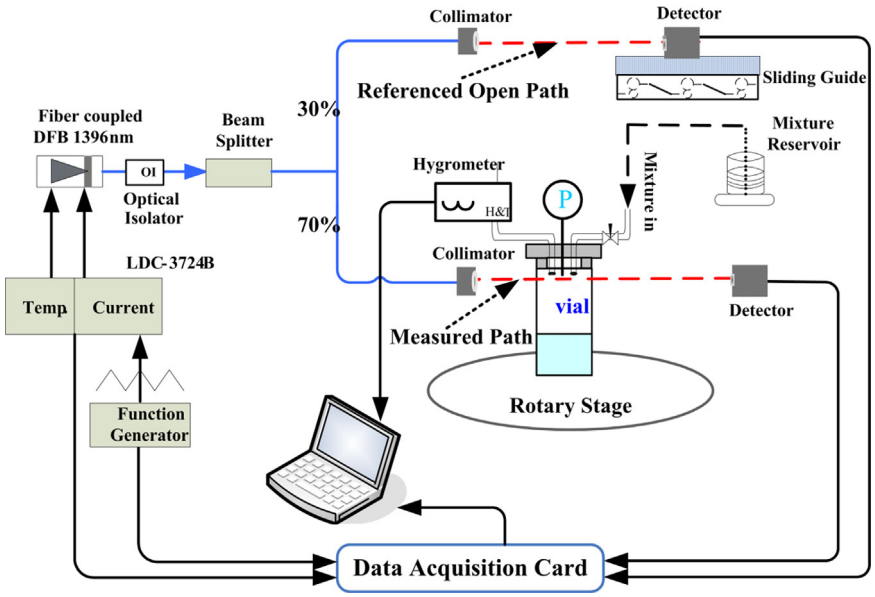

Fig. 1. Scheme of the experimental setup.

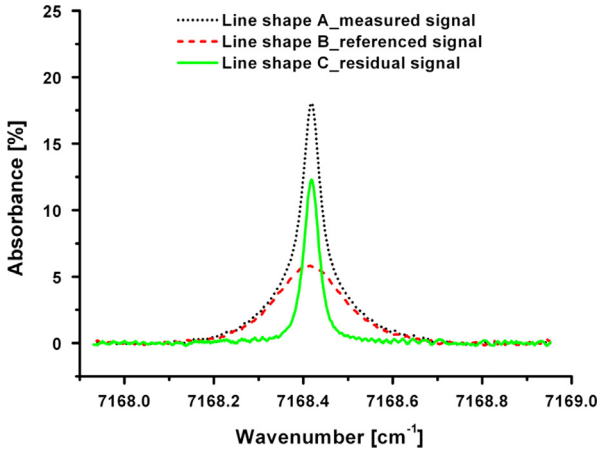

Fig. 2. The signals received from measurement path and reference path which are named as measured signal (A) and referenced signal (B) respectively. Pressure and H_2O concentration are inferred from the residual signal (C) which is the difference between measured and referenced signals.

can be adjusted precisely. The detector signals are sent through a low-pass analog filter before digital sampling by a multifunction data acquisition card (wwlab, MP4221, 12-bit A/D conversion) in a desktop PC. A procedure is written in LabView for data acquisition and analysis.

The sample cell used in the experiments is a cylindrical transparent glass vial with an inner diameter of 3 cm. The H_2O–air mixtures prepared in a stainless steel tank are delivered into the vial via stainless steel tubes. The tank and tubes are heated above the saturation temperature to ensure that all of the liquid water is evaporated. The gas pressures in the vial are measured by a vacuum pressure gauge (HongQi, ZB-150) with an accuracy of $\pm 0.1\%$ of reading and could be controlled precisely. A hygrometer (SENSIRION SHT75) placed at the vial exit is used to measure the relative humidity and the temperature of the gas. The absolute water–vapor concentration is then determined from these two values [32]. For H_2O measurements the absorbance profile is the results of the overlap of two lineshapes coming from ambient water vapor and the gas in the vial, as the lineshape "A" shown in Fig. 2. In order to prevent interference absorbance by ambient water vapor in the room air, the absorbance signal coming from ambient air (as the lineshape "B" shown in Fig. 2) is acquired and deducted from lineshape "A", and the residual lineshape "C" is the absorbance signal coming from the gas in the vial, which could be called as differential absorbance signal [33–35]. The remained signal is used to calculate the pressure and H_2O concentration in the vial. In our experiments, the lineshape "A" and "B" are computed from the measured signal and referenced signal respectively. Here it should be noted that in absorption spectroscopy the path length is the critical parameter when measuring gas concentration. In order to reduce the influence of ambient water vapor extensively, the path length of the referenced open path must be same as the length exposed in the ambient air of the measured path (difference between the length of the measured path and the external diameter of the vial).

4. Results and discussion

4.1. Measurements in static vial

A set of static vial experiments with controlled gas mixtures are performed to validate the sensor accuracy and reliability for the pressure and H_2O concentration derived from the absorbance signal "C". All experiments are performed with H_2O–air mixtures at room temperature. The line shape is least square fitted by a Voigt profile with the Doppler FWHM fixed at a value corresponding to the room temperature [31]. The pressure and H_2O concentration at the experimental conditions can be calculated according to Eqs. (3), (6) and (7) using the integrated absorbance and collisional FWHM provided by Voigt fit and the line strength ($S=0.2886\ \mathrm{cm^{-2}\,atm^{-1}}$) and pressure broadening coefficient ($\gamma_{air}=0.0946\ \mathrm{cm^{-1}/atm}$, $\gamma_{self}=0.4730\ \mathrm{cm^{-1}/atm}$) of the line listed in HITRAN2008 [36]. The reading of the pressure gauge and hygrometer are considered as references and used to compare with the measured values from the system.

The comparison between the pressure from the sensor and the vacuum pressure gauge readings is shown in Fig. 3. Correlation of those measured points has a square of the correlation coefficient $R^2=0.9973$, and the standard deviation is 1.23%. The results indicate that the pressures measured by the sensor ($P_{Measure}$) agree with the pressure gauge readings ($P_{Reference}$) over the tested pressure range of 10–760 torr (average bias $\sigma_P=|P_{Measure}-P_{Reference}|\sim 5.77$ torr).

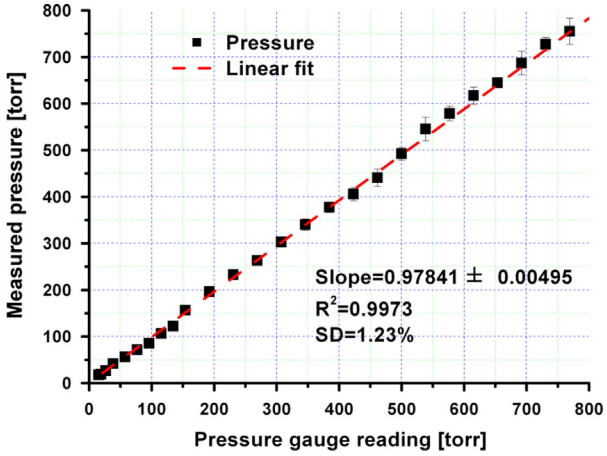

Fig. 3. Correlation between the measured pressure from the system and the vacuum pressure gauge readings in static vial.

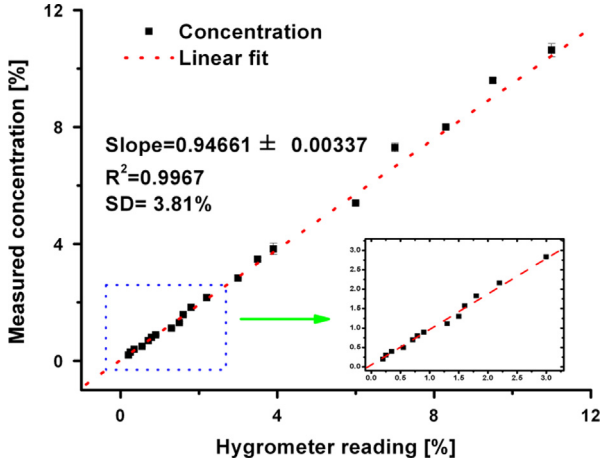

Fig. 4. Correlation between the H_2O mole fraction gained from the system ($x_{Measure}$) and the mole fraction obtained from hygrometer ($x_{Reference}$) in static vial.

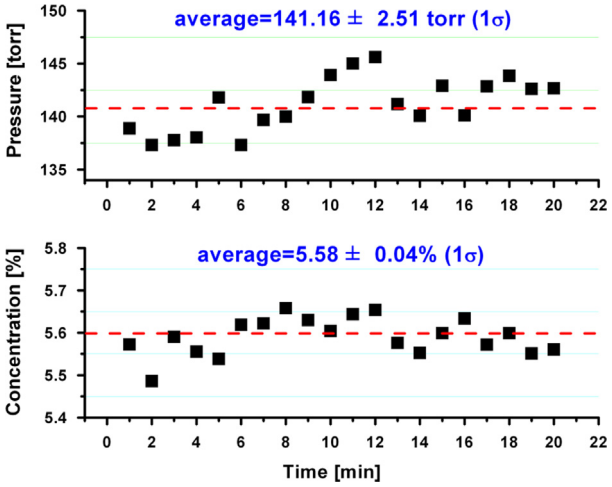

Fig. 5. Plots of 20 successive measurements in 20 min with 1 min interval for a gas mixture of 5.6% H_2O. The sensitivity which derived from the standard deviation of the 20 measurements is 440 ppm under 2.51 torr.

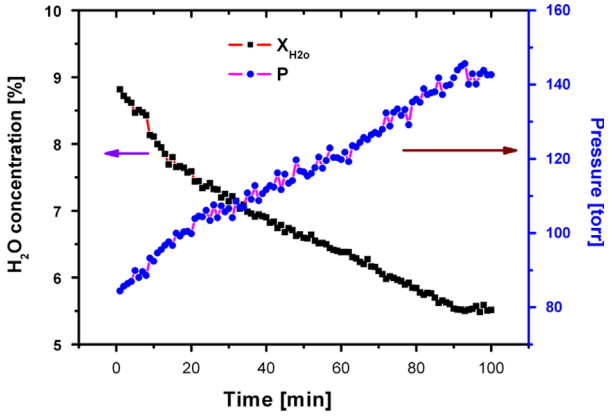

Fig. 6. Demonstration of uninterrupted leak detection for a vial which is sealed incorrectly over a period of 100 min.

Though it seems that error bars are bigger in the pressure range of 450–760 torr, the relative errors for each pressure are similar over the whole tested pressure range, the maximum being 5.54% and the mean being 2.09%. Fig. 4 shows the comparison of the H_2O mole fraction measured by the sensor ($x_{Measure}$) and the mole fraction measured by hygrometer ($x_{Reference}$). The correlation and standard deviation between the measured and actual H_2O mole fraction are 0.9967 and 3.81% respectively over the concentration range of 0.2–11%. The pressure and H_2O mole fraction from the sensor agree extremely well with the pressure gauge and hygrometer measurements. The errors in Figs. 3 and 4 primarily come from uncertainties in pressure measurements by pressure gauge, measured spectroscopic data, absolute water-vapor concentration inferred from the hygrometer reading and error in the baseline and line shape fits in the direct absorption measurements.

In order to evaluate the measurement sensitivity by calculating the variance of the average concentration, repeated measurements of a relatively low pressure and H_2O concentration of the gas mixture are performed. Because of the stable conditions during the estimated 20 min experiment, the gas pressure and H_2O concentration in the vial are assumed to be invariant. During this experiment, 20 successive measurements are performed with 1 min interval, each measurement taking ~300 ms. Fig. 5 shows 20 successive measurement results for a gas mixture of 141 torr pressure and 5.6% H_2O. The top graph shows the measured pressure with an average value of 141.2 ± 2.5 torr (1 standard deviation), indicating a sensitivity of 2.5 torr for the measurement of pressure. An average concentration of $5.58 \pm 0.04\%$ is yielded from those measurements, as shown in the bottom graph, indicating a sensitivity of 400 ppm over a 3 cm absorption path length.

An experiment with a vial which sealed incorrectly is performed to demonstrate ability of the sensor for uninterrupted leak detection. The initial headspace gas is composed of 8.8% water vapor and 91.2% nitrogen at 83.6 torr. The stopper of the vial is punctured with a needle to simulate a leak and the vial is stored in an air atmosphere. The headspace pressure and H_2O levels are then monitored over a period of 100 min. The results are shown in Fig. 6. It can be seen from the figure that as the air diffuses into the vial, the H_2O concentration decreases from 8.8% to 5.5% over the period, and the pressure rises from 83.6 torr to 143.6 torr. This experiment confirms the capability of the sensor for uninterrupted leak detection.

4.2. Demonstration on a rotary stage

In order to illustrate the potential of the sensor for in-line applications to the pharmaceutical industry, measurements are made on vials which are placed on a rotary stage to simulate the process of a assembly line. The radius of the rotary stage is 21 cm, and 30 vials are placed equally on the stage forming a circle. During the experiment, the rotating speed is 1.3 rad/s, once the laser beam hits the vial side, the laser changes its propagation and

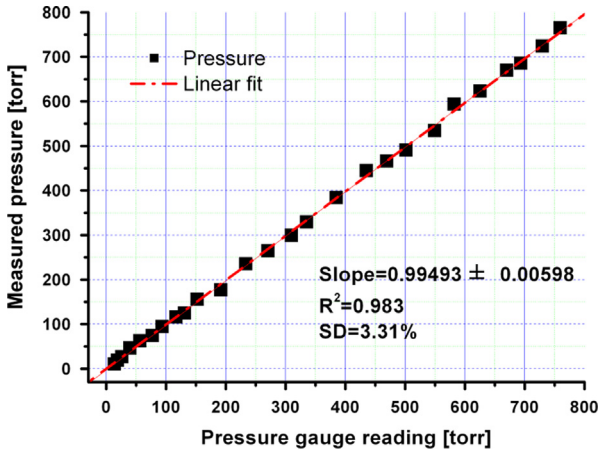

Fig. 7. Correlation between the measured pressure from the system and the vacuum pressure gauge readings for demonstration on a rotary stage which is used to simulate the in-line process.

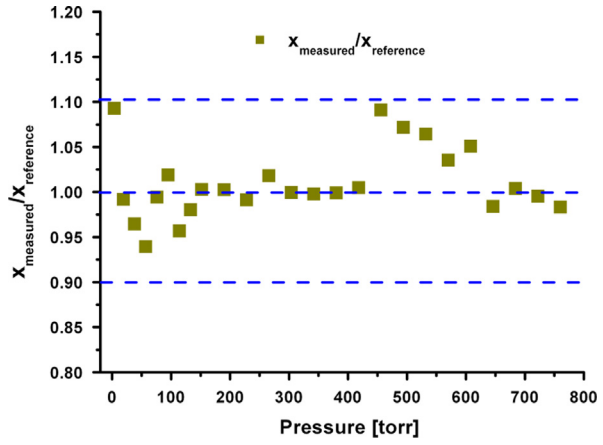

Fig. 8. The ratios of the H_2O concentration measured by the system ($x_{Measure}$) and the hygrometer reading ($x_{Reference}$) for the demonstration on a rotary stage.

the detector receives nothing. At the mean time, a trigger signal is sent to the DAQ card to start acquiring data after 50 ms, the data acquisition takes 21 ms (7 scans) and then stops to wait for the next vial. These two temporal parameters are selected based on the scanned frequency (333 Hz) of the triangle ramp and the rotational speed (1.3 rad/s) of the rotary stage. In this way the measurement can be performed at each vials' center within a range of $\pm$ 0.25 cm and 360 vials can be measured within 1 min. Fig. 7 shows the comparison of the pressure from the sensor with the vacuum pressure gauge readings. They are in good agreement over the tested pressure range of 10–760 torr. Correlation of those measured points has an R^2 value of 0.983, the standard deviation is 3.31%, and the average bias is $\sigma_P = |P_{Measure} - P_{Reference}| \sim 6.51$ torr). Fig. 8 shows the ratios of the H_2O mole fraction measured by the sensor ($x_{Measure}$) and the mole fraction measured by hygrometer ($x_{Reference}$). The standard deviation between the measured and actual H_2O mole fraction is 3.89%.

An experiment used to demonstrate the performance of the sensor for headspace pressure and H_2O concentration analysis of commercial freeze-dried products is also performed. In this experiment, thirty samples of commercial freeze-dried product are packaged in 10 ml vials and stoppered at 76 torr of nitrogen. One of the vials' stoppers is punctured with a needle and another is punctured 3 times with the same needle. All of the vials are stored in an air atmosphere for 2 h before the measurements. Those vials are arranged on the rotary stage and could be analyzed

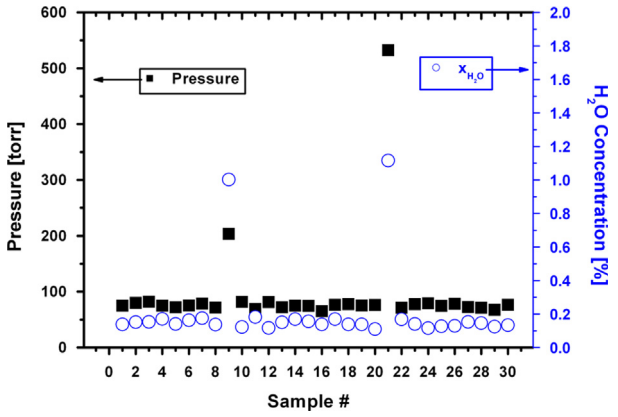

Fig. 9. Headspace pressure and H_2O concentration in 30 vials of commercial freeze-dried product. The specified pressure is 76 torr of nitrogen. Two vials leaked because their stoppers are punctured with a needle.

when they come across the measured beam as the stage rotates. As seen in Fig. 9, measuring the vacuum levels in the headspace shows that all of the containers still have the same pressure level with the initial stoppering state except the two whose stoppers are punctured with a needle. Because the hole size punctured on the two stoppers are different, the two vials have different headspace pressure levels (203 torr and 532 torr). It also can be seen from the figure that the elevated headspace H_2O levels of the two vials are nearly the same, because the ambient air leaked into the vials has the same water concentration.

In order to know the ability of the sensor, a comparison with other systems with same functions reported in references [27,28] are made in Table 1. Only pressure is measured in reference [27] and both pressure and moisture are measured in reference [28]. FMS scheme is employed for both systems in the two references. Some values used for comparison are obtained by calculation using the data listed in the references, for example, the deviation between $P_{Measure}$ and $P_{Reference}$ for references [27], the standard deviation between the measured and known values and the average sensitivity for the concentration measurement for references [28]. As illustrated in this table, the performance of our system is comparable with the other two systems which employing FMS scheme. Considering the simple construction and inexpensive of the system, our sensor is more suitable for industry application.

5. Conclusions

Non-intrusive measurements of pressure and H_2O concentration in the headspace of vials are demonstrated using TDLAS technique. In contrast to other headspace analysis systems based on TDLAS, a remained signal which is the difference between a measured signal and a referenced signal is used to infer the pressure and H_2O concentration in the vial. In this way the sensor does not need inert gas purges and calibration with known gas. Experiments for commercial freeze-dried products demonstrate the accuracy (3.31% for pressure and 3.89% for H_2O concentration) and in-line applications of the sensor for the pharmaceutical industry. Next we will confirm the capability of the sensor on the process of a real production line in a pharmaceutical factory and realize its industrialization. In addition, studies are now being extended to the measurements for non-transparent containers.

As a valuable diagnostic technology based on optical spectroscopy, it is obvious that the method is not limited to the pharmaceutical industry, or for the measurement of freeze-dried products. It can also be used in many other fields, such as food stuffs and packaging, wood-drying processes, cosmetic surgery,

Table 1
Comparison of the performance of our sensor with other systems with same functions.

Reference	Pressure measurement range	Coefficient of correlation for pressure measurement	Deviation between $P_{Measure}$ and $P_{Reference}$ (%)	Pressure sensitivity	Deviation between $x_{Measure}$ and $x_{Reference}$	x_{H_2O} sensitivity
[27]	0.04–0.5 atm	0.99	1.05	NT	NT	NT
[28]	0–1 atm	0.996	2.94%	2.2 torr	4.05%	0.00967 torr
This work	0.01–1 atm	0.983	3.31%	2.5 torr	3.89%	$141.2 \times 5.6\% \times 0.04\% = 0.00316$ torr

NT = not tested.

water activity measurement, water-holding capacity of solids, moisture permeability studies, and so on. The potential of the method in these fields will also be illustrated in the future.

Acknowledgments

This research is funded by the National Natural Science Foundation of China (No. 11104237), the Open Research Fund of Key Laboratory of Atmospheric Composition and Optical Radiation, Chinese Academy of Sciences (No. 2012JJ04) and the Education Committee Foundation of Jiangsu Province (No. 11KJB140010).

References

[1] Pikal MJ. Freeze drying. Encyclopedia of pharmaceutical technology. New York: Marcel Dekker; 2002; 1299–326.
[2] Skrabanja ATP, De Meere ALJ, De Ruiter RA, Van den Oetelaar PJM. Lyophilization of biotechnology products. PDA J Pharm Sci Technol 1994;48:311–7.
[3] Cameron P. Good pharmaceutical freeze-drying practice. Buffalo Grove: Interpharm Press, Inc.; 1997.
[4] Pikal MJ, Shah S. Intravial distribution of moisture during the secondary drying stage of freeze drying. PDA J Pharm Sci Technol 1997;51:17–24.
[5] Schneid SC, Gieseler H, Kessler WJ, Luthra SA, Pika MJ. Optimization of the secondary drying step in freeze drying using TDLAS technology. AAPS Pharm Sci Tech 2011;12:379–87.
[6] Connelly JP, Welch JV. Monitor lyophilization with mass spectrometer gas analysis. J Parenter Sci Technol 1993;47:70–5.
[7] Bardat A, Biguet J, Chatenet E, Courteille F. Moisture measurement: a new method for monitoring freeze-drying cycles. J Parenter Sci Technol 1993;47:293–9.
[8] Genin N, René F, Corrieu G. A method for on-line determination of residual water content and sublimation end-point during freeze drying. Chem Eng Process 1996;35:255–63.
[9] Nail SL, Johnson W. Methodology for in-process determination of residual water in freeze-dried products. International symposium on biological product freeze-drying and formulation Bethesda. Dev Biol Stand 1991; 74:137–51.
[10] Milton N, Pikal MJ, Roy ML, Nail SL. Evaluation of manometric temperature measurement as a method of monitoring product temperature during lyophilization. PDA J Pharm Sci Technol 1997;51:7–16.
[11] Remmele RL, Stushnoff C, Carpenter JF. Real-time in situ monitoring of lysozyme during lyophilization using infrared spectroscopy – dehydration stress in the presence of sucrose. Pharm Res 1997;14:1548–55.
[12] Mackenzie AP. Apparatus for microscopic observations during freeze-drying. Biodynamica 1964;9:213–22.
[13] Marques MJP, Loch LC, Wolff E, Rutledge DN. Monitoring freeze drying by low resolution pulse NMR: determination of sublimation endpoint. J Food Sci 1991;56:1707–10.
[14] Cavatur RK, Suryanarayanan R. Characterization of phase transitions during freeze-drying by in situ X-ray powder diffractometry. Pharm Dev Technol 1998;3:579–86.
[15] Allen MG. Diode laser absorption sensors for gas-dynamic and combustion flows. Meas Sci Technol 1998;9:545–62.
[16] Hanson RK, Jeffries JB. Proceedings of the 25th AIAA aerodynamic measurement technology and ground testing conference, American Institute of Aeronautics and Astronautics, AIAA 2006-3441.
[17] Persson L, Gao H, Sjöholm M, Svanberg S. Diode laser absorption spectroscopy for studies of gas exchange in fruits. Opt Laser Eng 2006;44:687–98.
[18] Shemshad J, Aminossadati SM, Kizil MS. A review of developments in near infrared methane detection based on tunable diode laser. Sensor Actuat B-Chem 2012;171–172:77–92.
[19] Bone SA, Cummins PG, Davies PB, Johnson SA. Measurement of water vapor pressure and activity using infrared diode laser absorption spectroscopy. Appl Spectrosc 1993;47:834–43.
[20] Gieseler H, Kessler WJ, Finson M, Davis SJ, Mulhall PA, Bons V, et al. Evaluation of tunable diode laser absorption spectroscopy for In-Process water vapor mass flux measurements during freeze drying. Pharm Technol 2007;96:1776–1793.
[21] Schneid SC, Gieseler H, Kessler WJ, Pikal MJ. Non-invasive product temperature determination during primary drying using tunable diode laser absorption spectroscopy. J Pharm Sci 2009;98:3406–18.
[22] Kuu WY, Nail SL, Sacha G. Rapid determination of vial heat transfer parameters using tunable diode laser absorption spectroscopy (TDLAS) in response to step-changes in pressure set-point during freeze-drying. J Pharm Sci 2009;98:1136–54.
[23] Lundin P, Cocola L, Lewander M, Olsson A, Svanberg S. Non-intrusive headspace gas measurements by laser spectroscopy – performance validation by a reference sensor. J Food Eng 2012;111:612–7.
[24] Priyadarshini C, Somsubhra G, Sathis KD, Parthiban N, David B. Frequency modulation spectroscopy: a review. Int J Biol Pharm Res 2012;32:82–8.
[25] Isobel AC, Kevin RW. Headspace moisture mapping and the information that can be gained about freeze-dried materials and processes. PDA J Pharm Sci Technol 2011;65:457–67.
[26] Mahajan R, Templeton AC, Han YR. Rapid headspace oxygen analysis for pharmaceutical packagaing applications. Pharm Technol 2002;7:44–61.
[27] Lin TP, Hsu CC, Kabakoff BD, Patapoff TW. Application of frequency-modulated spectroscopy in vacuum seal integrity testing of lyophilized biological products. PDA J Pharm Sci Technol 2004;58:106–15.
[28] ⟨http:/www.lighthouseinstruments.com/index.php?pid=30&lang=en⟩.
[29] Jenkins TP, Berg T. Diode laser absorption sensor for detecting oxygen in head space of vials, in: Proceedings of the IEEE sensors conference, 2008; p. 266–9.
[30] Demtroder W. Laser spectroscopy. 3rd ed. New York: Springer; 2003.
[31] Whiting EE. New empirical approximation to the Voigt profile. J Quant Spectrosc Radiat Transf 1976;16:611–4.
[32] ⟨http:/www.cactus2000.de⟩.
[33] Mount GH, Rumburg B, Havig J, Lamb B, Westberg H, Yonge D, et al. Measurement of atmospheric ammonia at a dairy using differential optical absorption spectroscopy in the mid-ultraviolet. Atmos Environ 2002;36:1799–1810.
[34] Sun X, Ewing DJ, Ma L. A laser extinction based sensor for simultaneous droplet size and vapor measurement. Particuology 2012;10:9–16.
[35] Corsi C, D'Amato F, De Rosa M, Modugno G. High-resolution measurements of line intensity, broadening and shift of CO2 around 2 μm. Eur Phys J D 1999;6:327–32.
[36] Rothman LS, Gordon IE, Barbe A, Benner DC, Bernath PE, Birk M, et al. The HITRAN 2008 molecular spectroscopic database. J Quant Spectrosc Radiat Transf 2009;110:533–72.